Feasibility studies of a novel extrusion process for curved profiles:

Zhou, Wenbin; Lin, Jianguo; Dean, Trevor A.; Wang, Liliang

DOI:
10.1016/j.ijmachtools.2017.12.001

Document Version
Peer reviewed version

Citation for published version (Harvard):
Zhou, W, Lin, J, Dean, TA & Wang, L 2018, 'Feasibility studies of a novel extrusion process for curved profiles: Experimentation and modelling', *International Journal of Machine Tools and Manufacture*, vol. 126, pp. 27-43. https://doi.org/10.1016/j.ijmachtools.2017.12.001

Accepted Manuscript

Feasibility studies of a novel extrusion process for curved profiles: Experimentation and modelling

Wenbin Zhou, Jianguo Lin, Trevor A. Dean, Liliang Wang

PII: S0890-6955(17)30177-3

DOI: 10.1016/j.ijmachtools.2017.12.001

Reference: MTM 3314

To appear in: *International Journal of Machine Tools and Manufacture*

Received Date: 9 July 2017

Revised Date: 3 October 2017

Accepted Date: 1 December 2017

Please cite this article as: W. Zhou, J. Lin, T.A. Dean, L. Wang, Feasibility studies of a novel extrusion process for curved profiles: Experimentation and modelling, *International Journal of Machine Tools and Manufacture* (2018), doi: 10.1016/j.ijmachtools.2017.12.001.

Feasibility studies of a novel extrusion process for curved profiles: Experimentation and modelling

Wenbin Zhou[a], Jianguo Lin[a,*], Trevor A. Dean[b], Liliang Wang[a]

[a]*Department of Mechanical Engineering, Imperial College London, London SW7 2AZ, UK*

[b]*Department of Mechanical Engineering, University of Birmingham, Birmingham B15 2TT, UK*

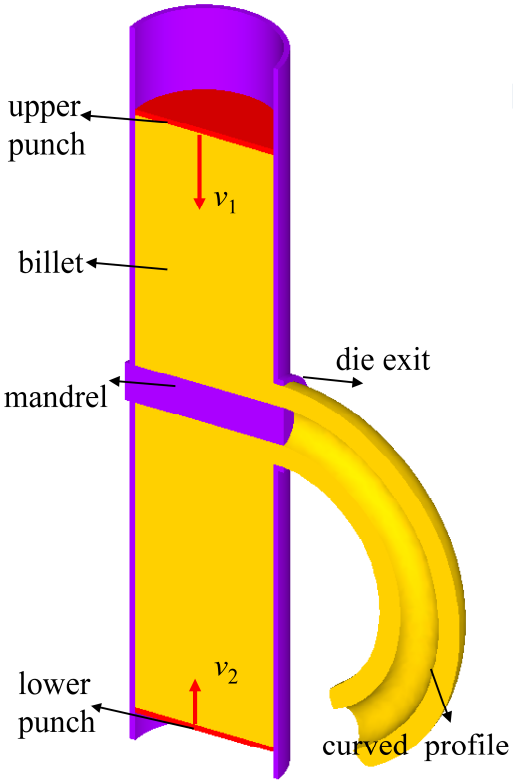

cross-sections of mandrel and die exit fabricating curved profiles with thickness $t=(D_2-D_3)/2$

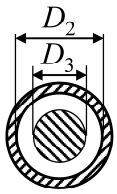

active control of v_2/v_1 to achieve adjustable profile curvature

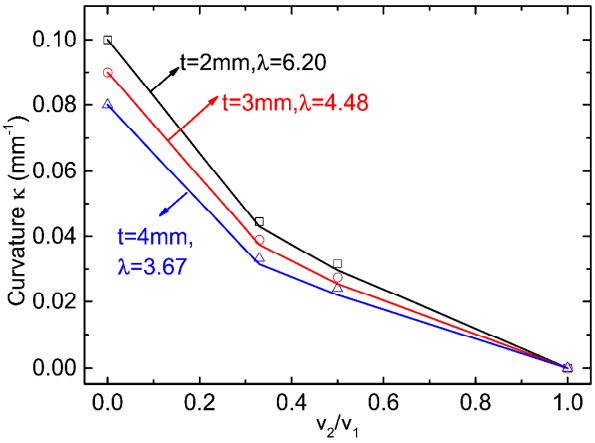

Feasibility studies of a novel extrusion process for curved profiles: Experiments and modelling

Abstract

The work described in this paper concerns a novel method for directly forming curved profiles/sections from billets in one extrusion operation using two opposing punches. Its mechanics are based on internal differential material flow, and it has been given the acronym, differential velocity sideways extrusion (DVSE). A tool set enabling sideways extrusion to be performed using opposing punches moving with different velocities was used for a series of experiments in which punch velocity ratio and extrusion ratio were process parameters. Plasticine was used as a model work-piece material and a series of compression tests were undertaken, to determine its constitutive properties and gain an estimate of work-piece die friction for use in process simulation. Curvature of extrudate can be controlled and varied using a difference between the velocities of the two punches, defined by velocity ratio. Greater curvature is achieved with lower velocity ratio. Curvature is also dependent on extrusion ratio, an increase in which increases curvature, although curvature is less sensitive to it than to velocity ratio. The extent of work-piece flow velocity gradient across the die exit orifice, which causes curvature, has been identified. Severe plastic deformation of the extrudate occurs in a way similar to channel angular extrusion (CAE), thus a greatly promoted effective strain level is achieved, though it is not always uniform across a section. The inner bending region of an extrudate experiences maximum localised effective strain, which decreases with decrease in curvature. To the authors' knowledge this is the first publication in which extrudate curvature is deliberately induced using opposing punches with differential velocities. Although only fixed velocity ratio values have been used in the work described in this paper the ability to change during operation exists and the process has the potential for the production of a profile with different curvature along its length.

Keywords: Profiles/Sections; Bending; Curvature; Severe Plastic Deformation (SPD); Sideways Extrusion; Channel Angular Extrusion (CAE)

1. Introduction

Aluminium alloy has a wide range of application for structural components in both aerospace and automotive industries, on account of its good combination of light weight and high strength. Reduced fuel consumption and therefore decreased CO_2 emissions can be achieved by utilising lightweight aluminium components in aircraft, trains and cars. In industry, ultra-light structures of complicated design have been manufactured using extruded aluminium alloy profiles with various complex cross-sections, which possess high stiffness and strength. Since sculptured forms can readily be achieved with aluminium profiles using simple machining and welding, efficient lightweight, capacious aerodynamic transportation modules can be produced at low cost. [1-4]. Considering the high demand for reducing weight and aerodynamic resistance, as well as improving aesthetics, in high-speed transport systems, an ability to manufacture accurate, high strength, hollow sections, longitudinally curved, in large quantity at low cost is opportune.

Since the beginning of the twentieth century, various forming techniques for curved profiles have been proposed. They mainly consist of known cold forming operations such as stretch bending, press bending, rotary draw bending and roll bending. Much research has been undertaken to refine these operations [5-10], however, intrinsic problems such as cross-sectional distortion and springback remain to be controlled using secondary operations and the tools are expensive, thus significantly increasing manufacturing cost and decreasing productivity. Some novel stress superposed cold bending techniques, i.e. torque superposed spatial (TSS) bending and superposed three-roll-bending with subsequent profile deflection, have been proposed to alleviate these deficiencies [11-15] and it has been shown that cross-sectional distortion and springback of curved profiles can be greatly reduced by superposition of torsion or compressive stress with external bending moment.

Several novel extrusion-bending integrated methods for forming curved profiles have been developed, one is based on external bending apparatus to influence material flow at die exit orifice during the extrusion process. Curved profile extrusion (CPE) was proposed by Kleiner *et al.* [16,17] to reduce forming stages in the manufacture of curved profiles. During CPE the metal billets are formed into curved profiles using consecutive extrusion and bending stages, thus significantly improving manufacturing efficiency. A curved profile is obtained by installing a bending device (guiding tool) immediately behind the die exit (hold by the backup plate) which deflects the extrudate to the prescribed value of curvature, as illustrated in **Fig. 1a**. CPE was further developed by Muller *et al.* [18,19], who achieved curvature with a segmented regulating guiding device composed of serially placed bending discs at the die exit, as shown in **Fig. 1b**. The discs could be

adjusted prior to extrusion to give a specified curvature. Another method for obtaining curvature is by introducing asymmetry in the metal flow, by tool design. Using this concept, Shiraishi *et al.* [20-22] developed a novel extrusion-bending method for producing curved bars and tubes, in which a billet is extruded through a die orifice with its axis inclined towards the central axis of the container (see **Fig. 1c**). Experiments were carried out using plasticine as work-piece material and it was found that by adjusting the inclination angle of the die exit orifice, material flow velocity across the die exit orifice can be regulated to produce curvature of extruded bars and tubes. It was found that curvature increases with increase of inclination of the die and also is affected by extruded profile geometry. Dajda *et al.* [23] proposed using an eccentrically positioned mandrel and eccentric die orifice to extrude pipe bends and elbows. Curvature was achieved through the derived asymmetric flow field in the region of the orifice. Chen *et al.* [24] studied the influence of extrusion ratio, and eccentricity ratio of holes on curvature of aluminium alloy 7075 profiles produced by multi-hole extrusion, in which a billet is extruded by a single punch through either a two-hole or three-hole die (see **Fig. 1d**). It was found that the eccentricity ratio of the die orifices is the most critical factor affecting curvature which increases with increasing eccentricity ratio.

It is apparent that profile curvature extruded using the methods described above, has essentially a pre-set constant value. In this paper, a novel extrusion method termed, differential velocity sideways extrusion (DVSE), in which two punches are utilised, is proposed, to extrude billets directly into curved sections within one single operation. The novelty of this process exists in that a difference in velocity between the two punches is used to control curvature and that curvature can be changed by changing the ratio of punch velocities within a continuous operation.

Sideways extrusion (also known variously as either; ‘lateral’, ‘radial’, ‘cross’ or ‘transverse’ extrusion), is a class of extrusion in which a billet is pressed in a cylindrical chamber by a punch or by two opposing punches, and contrary to the axial flow of conventional extrusion, flows radially (normal to the extrusion chamber) outwards through an aperture. Previous research has been undertaken in which the process has taken various forms [25-27]. The extrusion aperture is used to guide the extrudate to ensure it is straight and normal to the billet axis and it can be used for forming parts from either solid or hollow billets. **Figure 2a** shows three tooling configurations for extruding solid and hollow side arms from a solid billet [27]. This basic tooling design is commonly employed for producing straight solid/tubular components (rod, tube, cup) whose cross sections are decided by the die opening/orifice and the mandrel. Rudolf [28] proposed a development for forming asymmetric tubular parts using tubular billets and mandrels (see **Fig. 2b**). A lateral punch system is used to provide an additional horizontal tool axis acting as the mandrel. Wälder *et al.* [29] further developed Rudolf’s process for asymmetric cup parts using tubular billets (see **Fig. 2b**). The

cup was formed without an additional horizontal tool axis (mandrel), making it possible to lower the tool design's complexity and cost, however, roundness deviation and wall thickness deviation were found. Both authors concluded that the synchronous movement of the upper and lower halves of the closing die device is essential to achieve straight tube/cup.

Injection forging, or radial forging, see **Fig. 2c**, (so called because the lateral feature is machined into the side of a container and is not developed by approaching top and bottom dies, as in conventional closed-die forging) is a near-net or net-shape completely closed-die, net-shape process for producing components with central bodies and lateral features. The features can be axisymmetric, such as for gears, splines, arms on CV joint spiders, inner races and flanges, or asymmetric such as for cams and levers. A single punch or two opposed punches moving co-axially inside a chamber force a work-piece to flow radially into an annular space which is normally closed [30-32]. Injection forging is referred as sideways extrusion by some researchers due to a similarity of flow fields [33-35], especially for a forging die cavity/land with an opening/orifice [35]. However strictly speaking they are different, since the lateral feature is fully constrained by a die in injection forging whereas it is unconstrained in extrusion. Largely to demonstrate the effect of container friction on die filling, previous tool designs for injection forging lateral features have included single punches, twin punches and fixed or moving containers [35,36]. Although the effect of direction of movement of the work-piece in the container has been recognised, little work to quantify the effect of punch velocity difference on solid parts forged in closed dies has been undertaken [35,37]. Alves *et al*. [35] studied the effect of the kinematics of the movable active tool components on the final geometry of injection forged components. The relative velocity between the movable upper punch and floating die was controlled with two different types of the spring closing elements having different spring constants, while the lower punch was fixed (see **Fig. 2d**). They found that using a double-acting tool with punches of equal speed, obviates bending defects occurring in a tool in which relative top and bottom punch velocities were different. Johnson *et al.* [37] gave a simple possible slip-line field for a closed die forging in double-sided compression under plane strain conditions (neglecting die lands), and concluded that for free sideways expulsion of solid forged parts into die lands the two slip-line fields must be of the same shape, irrespective of the relative velocities of the two punches.

In much of the research work on injection forging described above, the effect of container friction on metal flow has been implicitly recognized and partially mitigated by the use of opposing punches and moving containers, but to the authors' knowledge no work in which prescribed velocities of opposing punches to deliberately induce curvature in laterally extruded (as opposed to

forged) features has been published. Contrarily, tooling has always constrained metal flow to a radial path. Also, curved extrudates have been obtained in tooling containing single punches.

The work described in this paper concerns a tool set and methodology, with the acronym DVSE, for producing controlled and possibly varied curvature, using a single container with opposing punches at each end and a lateral facing die orifice. A novel rig has been designed and manufactured to study the DVSE process. Experiments were conducted with plasticine, a commonly used model material for observing flow patterns in metal forming. Plasticine has been proved to be appropriate and widely used as physical model material for metal forming processes [38-41]. Being readily sectioned, it gives the opportunity to study material flow behaviour needed for tool design investigations. Effects of the extrusion velocity ratio of two opposing punches, and extrusion ratio (defined as the cross-sectional area ratio of the billet to that of the extruded profile), on the curvature of the formed profile were investigated in detail. A finite element programme has been used in parallel with experiments, to validate its accuracy and facilitate understanding of fundamental properties of the DVSE process. The findings are aimed to highlight the effect of forming parameters and procedures on the characteristics of extruded profiles.

2. Differential velocity sideways extrusion (DVSE)

2.1. Principle of DVSE

Figure 3 shows a schematic of differential velocity sideways extrusion (DVSE), where the initial situation is shown in **Fig. 3a**, and an intermediate forming stage in **Fig. 3b**. The profile is extruded sideways out of the container and its exiting direction is perpendicular to the punch motion direction. The basic principle of this method is that profiles are extruded and bent simultaneously, due to the gradient of the internal material flow velocity over the die exit caused by the different relative moving velocities of the two extrusion punches. It is expected that by adjusting the extrusion velocity ratio of the two punches as well as the extrusion ratio, curved metal profiles/sections with adjustable arbitrary curvatures can be formed in one extrusion-bending procedure.

2.2. Extrusion rig design

Figure 4 shows the tool set designed and manufactured for undertaking differential velocity sideways extrusion (DVSE). Split extrusion dies and chambers were utilized in the present study to facilitate easy and quick removal of the extruded profiles, for examination of flow patterns, as shown in **Fig. 4a**. The chamber for the billet was 25.6mm in diameter and 150mm in height. A mandrel installed on the container wall opposite to the die exit orifice, was used for extruding

hollow sections. The dies were designed to extrude round billets into profiles with circular cross-sections, thus the die exit orifice and mandrel were circular. The length of an extrusion die bearing land normally falls within 1~3mm for soft metal (Al, Cu etc.) and 2~4mm for carbon steel [42], here 2mm is used, which was chosen to ensure sufficient strength and small frictional effect on material flow. The extrusion dies were made of AISI type H13 hot work tool steel hardened and tempered to 50HRC. Dimensions of the tool are listed in **Table 1**.

The extrusion tests were carried out on a 2500kN Instron universal hydraulic press, as shown in **Fig. 4b**. The velocity of the upper punch can be directly controlled by the universal hydraulic press, however, except for the situation where the extrusion velocity of the lower punch was zero, a specially designed multi-motion loading device was needed to achieve synchronisation and different extrusion velocity ratios of the lower punch v_2 to upper punch v_1 (v_2/v_1=0~1). A special double-action/motion loading rig was designed and manufactured, using the principle of crossed levers. This enabled the ratio of the velocity of the lower punch, v_2 to the velocity of the upper punch, v_1, to be varied as; v_2/v_1=0, 1/3, 1/2, 2/3, 1. It was mainly composed of four drive rods and four levers. The drive rods were used to transfer the motion of the upper punch to the levers, which then transferred the motion to the lower punch through the drive rods at the other end of the levers. In this way the motions of the upper punch and the lower punch were synchronized. By positioning the four drive rods which connected the upper and lower punches at different relative locations on the levers, the velocity of the upper punch v_1 can be transferred to the lower punch v_2 at different ratios. An illustration of the kinematics of the double-action loading rig is given in **Fig. 4c**, where the following relationship existed; $v_2/v_1 = v_{2p}/v_{1p}$=BC/AC=BB'/AA'. Both the upper and lower punches contained an adjustable front end in the perpendicular direction, which facilitated the alignment of the punch to the extrusion die chamber. The split extrusion die and double-action loading rig were assembled on a universal hydraulic press for DVSE tests.

3. Experimental method and simulation

3.1. Billet preparation

The material used for this investigation was plasticine. To ensure a reasonable degree of homogeneity, it was repeatedly rolled and folded, to consolidate it and remove any inner voids. Cylindrical billets were formed, 25.4mm diameter and 130mm high. A corresponding circular through-hole was cut along a diameter at half of the height of the billet for extrusion of the hollow round tube. The diameter of the hole was the same as that of the mandrel used, as given in **Table 1**. The preformed plasticine cylinder billets were relaxed at room temperature for four days to avoid any further changes in flow stress prior to use in tests. To enable deformation flow patterns to be

studied, some billets were cut in two along a diametral plane and square grids of 4mm×4mm were scribed on one of the two matching halves. A marker pen with coloured ink was used to highlight the grids. Finer grids of 2mm×4mm were scribed on the outer edge of the billet to reveal details in dead zones. The two halves were gently pressed together to form a cylindrical billet again for extrusion.

3.2. Work-piece/tool friction

The friction factor in the hot extrusion of metal is normally between 0.2 and 0.4 when graphite-based lubricants are used and between 0.7 and 1.0 without lubricant [43]. The friction factor in model tests and real process should be identical according to the similarity criteria [44]. Friction in metal forming is known to be a complex phenomenon, depending amongst other factors, temperature, pressure, surface spread, which vary throughout a process and no simple tests available to determine it. The compression ring test is the simplest means for obtaining a single value of friction and in spite of its limitations of little surface flow and modest surface pressure, it has been used widely by research workers. In this work several ring compression tests were conducted to identity friction values, using lubricants Vaseline and soap powder [40]. Plasticine ring samples of 36mm outside diameter, 18mm inside diameter and 12mm height (6:3:2) were prepared. Friction factors of 0.4 with soap powder and 0.1 with Vaseline were obtained, which were in accordance with the friction range identified from previous work [41]. It was also found that a thin layer of Vaseline covered with fine soap powder provided a friction factor of 0.3, which was closest to friction conditions, quoted for lubricated hot extrusion of metal. Therefore, this means of lubrication was selected for all the DVSE model tests.

3.3. Uniaxial compression tests

Uniaxial compression tests were conducted on plasticine specimens 30mm in high and 25mm diameter, to determine flow stress relations of plasticine. The compression tests were performed on a 250kN Instron universal testing machine. Vaseline was used as a lubricant and tests were carried out at strain rates of $0.01s^{-1}$, $0.05s^{-1}$ and $0.2s^{-1}$ and temperatures of 296K, 303K and 313K. A load cell was utilised to record the applied load, which was recorded at every 0.10mm travel of the cross-head until the final height of the specimen decreased to 15mm. The Norton-Hoff power law viscoplastic model was used to describe flow stress as [45]:

$$\sigma(\varepsilon, \dot{\varepsilon}, T) = Ke^{-\beta T}\varepsilon^{n}\dot{\varepsilon}^{m} \quad (1)$$

where T is absolute temperature, ε and $\dot{\varepsilon}$ are the effective strain and strain rate, respectively. β, n and m reflect the temperature sensitivity, strain sensitivity and strain rate sensitivity respectively.

The coefficients K, β, n and m of plasticine used in experiments were determined from the compression tests.

Figure 5 shows the true stress-strain curves of plasticine at strain rates of 0.01-0.25 and temperatures of 296 K, 303 K, and 313 K. Multiple tests were conducted to obtain the average value of experimental data for all strain rates and temperatures, which were then fitted to Eq. (1) to obtain the temperature sensitivity, strain sensitivity and strain rate sensitivity of plasticine. **Table 2** shows the fitted constants for the Norton-Hoff model, and comparisons between fitted curves (solid curves) and experimental data (hollow symbols) are illustrated in **Fig. 5**. It can be seen that the Norton-Hoff model fits experimental data well except for lower strain values ($\varepsilon \leq 0.15$), therefore like many metals at elevated temperatures the plasticine used here is a strain-hardening (n=0.15) and strain-rate-hardening (m=0.14) viscoplastic material, and the strain sensitivity (n) and strain rate sensitivity (m) values of plasticine are very close to those of aluminium and steels, whose strain rate sensitivity and strain-hardening values at elevated temperatures are in the range $0.10 \leq n \leq 0.25$ and $0.13 \leq m \leq 0.16$ [46-49].

3.4. Extrusion procedure

The experimental program undertaken is given in **Table 1**. The parameters varied during the experiment were the diameter D_2 of the die exit orifice, diameter D_3 of the mandrel, velocity v_2 of the lower punch. The wall thickness of the round tube was t=(D_2-D_3)/2. The velocity of the upper punch was fixed at v_1=1mm/s and velocity ratios v_2/v_1=0, 1/3, 1/2, 2/3, and 1 were obtained by different configurations of the double-action loading rig. Extrusion tests were carried out at room temperature, which was also the initial temperature of the billets and the extrusion tooling. At the start of each test the upper and lower punches were aligned and 10mm into the open top and bottom of the die chamber, which just contacted the top and bottom surfaces of the billet. At the end of each extrusion test, the split die was dismantled to remove the extruded profile.

3.5. Finite element analysis

A 3D finite element model was established using Deform-3D code. **Figure 6** shows the FE model of billet and DVSE tooling composed of two punches, a container, an exit die, and for hollow profile extrusion, a mandrel. Since the tooling was assumed to be rigid and only the billet was deformable, thicknesses of punch and container wall were simplified to be 1mm. The various dimensions of the mandrel and billet are the same as those used in experiments. Physical properties of billet and extrusion tooling materials are listed in **Table 3**. The similarity of flow behaviour between plasticine at room temperature and metal (steel, aluminium alloys) at elevated temperature

are discussed in Section 4.1. The flow stress data of AA6082 was imported into Deform-3D simulation using Zener-Hollomon model modified by Sheppard and Jackson as follows [50]:

$$\sigma(\dot{\varepsilon}, T) = \frac{1}{\alpha}\sinh^{-1}\left(\frac{\dot{\varepsilon}}{A}exp\left(\frac{Q}{RT}\right)\right)^{1/n} \quad (2)$$

where A and α are constants, n is stress exponent, Q is the activation energy, R is the universal gas constant and T is the temperature (K). **Table 4** shows the values of the material constants used in Zener-Hollomon model for AA6082 [46]. The initial temperature of both billet and die was 480^{o}C, and the surrounding environment temperature of the die was set as 300°C to reduce excessive heat loss caused by the simplified extrusion tooling [51]. The velocity of the upper punch was fixed at v_1=1mm/s, and velocity ratios v_2/v_1=0, 1/3, 1/2, 2/3, and 1 were simulated by varying the velocity of the lower punch as; v_2=0, 0.33, 0.5, 0.67, and 1mm/s. To decrease simulation time from the initial state to the steady state, the diameter of the billet was considered to be exactly the same as the inner diameter of the extrusion container, and thus no upsetting took place before the billet was extruded. Only a half portion of work-piece and tool was modelled using the advantage of its symmetry.

Both the extrusion tooling and billet in the FE model were meshed with tetrahedral elements. The absolute mesh density was used as the general meshing method, where the minimum size of an element was set as 0.5 mm and the size ratio was 2. A mesh window with an increased element density was applied to the aluminium billet around the mandrel and the die exit orifice to generate localised finer elements. The element size in this mesh window was set as 0.3 mm. A small relative interference depth of 0.3 was used to trigger the automatic remeshing procedure during the simulation process when the penetration depth between the element edges exceeded 30% of their original edge lengths. Friction at the billet-tooling interfaces was considered to be of shear type. The Shear friction model used was:

$$\tau = m\sigma/\sqrt{3} \quad (3)$$

where τ is the frictional shear stress, m $(0 \leq m \leq 1)$ is the friction factor and σ is the effective flow stress of the billet. In the present study, to ensure the similarity of flow behaviour between plasticine and hot metal, the same friction factor m=0.3 as the physical experiment was used in simulation.

4. Results and discussion

4.1. Extrusion of bar and tube

Profiles of round bars extruded with the same extrusion ratio (λ=1.61) and different extrusion velocity ratios of the lower punch v_2 to upper punch v_1 (v_2/v_1=0, 1/3, 1/2) are shown in **Fig. 7**. **Figure 8** contains profiles of tubes of circular ring section extruded with different thicknesses (t=2mm, 4mm, i.e. λ=6.20, 3.67) and extrusion velocity ratios (v_2/v_1=1/3, 1/2). The computed results from FEM are also illustrated for comparison. Two dashed concentric circles are overlaid on each of experimental and FEM result image to demonstrate the degree of circularity of the profiles, the diameters of the superposed circles are shown as well.

It can be seen from **Figs. 7-8** that FEM results agree well with the experimental results, thereby validating the numerical simulation results. The trial experiments using aluminium were carried out and shown in **Fig. 9**. The test condition was the same as that used in FEM, except that commercially pure aluminium AA1050 was used for trials. All extruded profiles are smoothly curved and circular and no defects in the cross-sections were detected, though each extrudate has a different curvature. The results suggest that the present extrusion process, differential velocity sideways extrusion (DVSE), is indeed feasible to directly form billets into curved solid and hollow profiles by one single extrusion-bending procedure, and degree of the curvature can be varied by changing both extrusion velocity ratio and extrusion ratio. Since it is a natural bending process based on internal differential material flow rather than external bending force, defects such as distortion and thinning of the cross-section are avoided and bending equipment, such as that used in conventional forming processes, is obviated.

4.2. Profile curvature

Relationships between the extrudate curvature, extrusion velocity ratio and extrusion ratio, for both round bars and tubes are illustrated in **Fig. 10**. The values of the curvature, plotted in the figures, were measured by fitting the experimental and simulation results to best-fit circles as shown in **Figs. 7-8**. Curvature is expressed as the inverse of the radius R_c. It can be seen from **Fig. 10** that extrusion ratio and velocity ratio v_2/v_1 both affect curvature. However, the effect of velocity ratio v_2/v_1 is more pronounced than that of the extrusion ratio. The effect of extrusion ratio is small when velocity ratio v_2/v_1 is greater than 0.5, below this value the effect of extrusion ratio increases as velocity ratio v_2/v_1 decreases. The curvature of bar and tube is reduced as the diameter D_2 of the die exit orifice increases, moreover for the same D_2 the curvature of the tube is reduced with increase of wall thickness of the tube, that is, lower extrusion ratio results in smaller curvature of both bars and tubes. Lower velocity ratio leads to greater curvature, and when velocity ratio v_2/v_1 is less than about 0.33, curvature of tubes increases significantly with reducing velocity ratio, while curvature

of bars varies relatively slowly with variation of extrusion velocity ratio. The maximum curvature of round bar of D_2=15mm (λ=2.87) at velocity ratio v_2/v_1=0 is 0.0288mm^{-1}, and the maximum curvatures of round tubes of thickness 2mm (D_2=15mm) and 2.5mm (D_2=20mm) at velocity ratio v_2/v_1=0 are 0.1mm^{-1} and. 0.095mm^{-1}, respectively.

Flow lines at the die orifice provide some understanding of the influence of the extrusion parameters on extrudate curvature and a comparison of velocity distribution for different extrusion ratios and velocity ratios, is shown in **Fig. 11**. The velocity ratio for **Figs. 11a-b,** is v_2/v_1=0. As shown in **Fig. 11a**, with extrusion ratio λ=2.87, velocity is higher at the upper orifice edge closer to the faster moving upper punch at 4.0 mm/s (line H) and decreases to 2.2 mm/s (line A) towards the lower orifice edge. At a lower extrusion ratio λ=1.61, as shown in **Fig. 11b**, velocity at the upper orifice edge is lower at 2.6 mm/s (line H) and decreases to 1.22 mm/s (line A) at the lower edge. Therefore, greater extrusion ratio leads to an increased velocity gradient at the orifice and thus greater curvature. It should be noted that the average material flow velocity at the orifice for the case of λ=2.87 is also greater than that for λ=1.61, due to the decrease of cross-sectional area of the orifice. The extrusion ratio in **Figs. 11b-d,** is the same and is λ=1.61. It can be seen that the velocity gradient decreases as v_2/v_1 increases, thus leading to a decreased bending curvature of the extrudate. When v_2/v_1=1, this velocity gradient becomes quite small and negligible considering the existence of numerical calculation error, as can be seen in **Fig. 11d** a straight profile is formed. It should be pointed out that the average material flow velocity at the die exit orifice increases as v_2/v_1 increases, due to the increase of the sum of extrusion velocities v_2 and v_1, though v_1 is fixed at 1mm/s.

4.3. Plastic deformation characteristics

Figure 12 shows grid distortions on extruded plasticine bars and simulated velocities, highlighting the dead zone are shown in **Fig. 13**. Here a velocity of 0.05 mm/s is used to define the upper flow limit of material in dead zone. As shown in these figures, a dead zone of roughly triangular shape, exists on the chamber wall opposite the die exit orifice. The dead zone extends as velocity ratio reduces and extends completely across the chamber when it is zero. In this situation, the tip of the triangle coincides with the die exit orifice and the volume of the workpiece between the slower punch and the orifice does not deform. To quantitatively study the effect of velocity ratio and extrusion ratio on dead zone, a dividing line passing through the vertex of the triangular dead zone is drawn in **Fig. 12**, which divides the deformation zone and die exit channel into two parts, namely e and D_2-e, the material flowing into these two parts to compose the extrudate comes from the corresponding two extrusion punches. Further, the eccentricity ratio $\hat{e}$ is employed to define the degree of deviation between the dividing line and the central line of die exit channel as follows:

$$\hat{e} = e/D_2 \quad (4)$$

where e is the distance between the dividing line and the boundary extension line of the exit channel closer to the faster punch, D_2 is the diameter of the exit channel, $0.5 \leq \hat{e} < 1$ is a normalised dimensionless variable. The obtained e and $\hat{e}$ are shown in **Figs. 14a-b**, respectively. It can be seen that a good agreement is achieved between experimental and FEM results. Lower velocity ratio v_2/v_1 and greater extrusion ratio λ lead to a greater eccentricity ratio $\hat{e}$ of the dividing line. As v_2/v_1 decreases, the dividing line moves towards the side which has a lower extrusion velocity (v_2), and when v_2/v_1=1 the dividing line is exactly in the centre of the die exit. The difference of $\hat{e}$ for λ=2.87 and λ=1.61 increases as the decrease of v_2/v_1, especially when $v_2/v_1 < 0.5$. This accords with the results in **Fig. 10** that the effect of extrusion ratio on the extrudate curvature is small when velocity ratio v_2/v_1 is greater than 0.5, below this value the effect of extrusion ratio increases as velocity ratio decreases.

The distortion of the grid in **Fig. 12** also indicates that asymmetrical material flow occurs near the die exit. The effective strain contour is illustrated in **Fig. 15,** which is in good agreement with the extent of grid distortion. The curved profile has experienced high effective strain levels which increase with extrusion ratio. This is similar to the severe plastic deformation (SPD) arising in equal or non-equal channel angular extrusion (ECAE or NECAE) processes. The strains arising in DVSE extrudates are not uniform across their sections, especially when the curvature is greater. The highest value of strain occurs in a thin inside region of the curved profile. As discussed before, the extrudate material comprises that provided by the two punches, the relative amounts being in proportion to their velocities. A greater effective extrusion ratio exists in the region (D_2-e) which is bounded by an extended dead zone dividing line nearer to the orifice edge and this is where strains will be greater. With lower velocity ratio v_2/v_1 and greater extrusion ratio, i.e. greater curvature, the eccentricity ratio increases while this thin region (D_2-e) narrows, leading to more severe plastic deformation for the inside bending region of the profile closer to the slower punch and less plastic deformation for the outside bending region closer to the faster punch. When v_2/v_1=1, the eccentricity ratio is 0.5 and the plastic deformation over the cross-section becomes symmetric, the effective strain distribution becomes reasonably homogeneous. It has been proven that a single pass of ECAE of aluminium alloy can refine grain structure and increase mechanical properties significantly, further ECAE processing only results in slight improvement, and reasonably homogeneous microstructure can be achieved as well after a single extrusion [52,53].

To compare with experimental results quantitatively, the effective strain is also calculated from **Fig. 12.** For a NECAE die without rounding of the corners at the intersection of the channels, the simple shear model gives the value of shear strain in one pass as [54]:

$$\gamma = \cot\alpha + \cot\beta \quad (5)$$

where α and β are the angles of the intersection plane with the entry and exit channels, respectively. For a 90 degree NECAE die, the value of equivalent strain can be calculated from Eq. (5) as:

$$\varepsilon = \gamma/\sqrt{3} = (q/w + w/q)/\sqrt{3} \quad (6)$$

where q and w are diameters of the entry channel and the exit channel, respectively**.** Here, $q = D_1 = 25.6\text{mm}$ is the same for all velocity ratios and extrusion ratios, however, as discussed before the die exit can be divided into two parts, which change with the variation of velocity ratio v_2/v_1 for a given extrusion ratio λ. Only the effective strain of outside bending part of the profile is calculated here, thus *e* shown in **Fig. 14a** is taken as *w* in Eq. (6). The comparison of calculated effective strain from experiment by using Eq. (6) and FEM is shown in **Fig. 16**. Since bending occurs with shear deformation, to minimise the effect of bending on element deformation, only the effective stain in the neutral plane (~1/2 *e*) of the outside bending part of the profile is extracted from FEM. The areas above and below the neutral plane have almost equal effective strains which are greater than that of the neutral plane, as shown in **Fig. 15**. It can be seen that the effective strain obtained from FEM is slightly greater than that of experiment, though the bending curvature obtained from FEM is slightly lower than that of experimental results. This may be due to the fact that Eq. (6) is essentially obtained from the simple shear model where only shear strain is considered during the deformation zone of ECAE or NECAE, also it is actually more applicable to the plane strain case where the width of the billet is not considered, however the DVSE is a three dimensional extrusion process where the width of the profile and the billet is not equal here, and bending is accompanied with extrusion as well. As can be seen in **Fig. 16**, the difference between experimental and FEM results decreases as the decrease of extrusion ratio and the increase of velocity ratio v_2/v_1, namely as the decrease of the extrudate curvature.

5. Conclusions

A novel method of forming controlled curved profiles/sections, differential velocity sideways extrusion (DVSE), has been proposed and verified through physical experiment and numerical modelling. The method essentially is sideways extrusion from a cylindrical container using opposing punches. The relative movement of slower to faster punch is defined by extrusion velocity ratio v_2/v_1 (0~1). It was found that DVSE can directly form billets into curved profiles without defects in the cross-sections by a combined extrusion-bending operation. Curvature of extrudates can be adjusted by varying the extrusion velocity ratio of the two extrusion punches as well as the extrusion ratio. Lower velocity ratio and greater extrusion ratio tend to increase the material flow velocity gradient at the die exit orifice and result in greater curvature. The effect of extrusion ratio is

less remarkable compared with extrusion velocity ratio, which also decreases as the extrusion velocity ratio increases. A curved extrudate has resulted in an enhanced effective strain level which increases as the increase of the extrusion ratio, as severe plastic deformation (SPD) arises, though it is not always uniform. For a given extrusion ratio, the maximum value of localised effective strain occurs near the inner bending region of the profile, and decreases with the decrease in curvature, namely increase of the velocity ratio, while the effective strain of its outside bending region increases as the curvature decreases.

Acknowledgement

The financial support from the President's PhD Scholarship Fund of Imperial College London, is greatly appreciated.

References

[1] J. Jeswiet, M. Geiger, U. Engel, M. Kleiner, M. Schikorra, J. Duflou, R. Neugebauer, P. Bariani, S. Bruschi, Metal forming progress since 2000, CIRP Journal of Manufacturing Science and Technology 1 (2000) 2-17.

[2] S. Chatti, U. Dirksen, M. Schikorra, M. Kleiner, System for design and computation of lightweight structures made of bent profiles, Advanced Materials Research 6 (2005) 279-286.

[3] M. Hermes, D. Staupendahl, C. Becker, A.E. Tekkaya, Innovative machine concepts for 3D bending of tubes and profiles, Key Engineering Materials 473 (2011) 37-42.

[4] A.E. Tekkaya, N.B. Khalifa, G. Grzancic, R. Hölker, Forming of lightweight metal components: Need for new technologies, Procedia Engineering 81 (2014) 28-37.

[5] F. Paulsen, T. Welo, A design method for prediction of dimensions of rectangular hollow sections formed in stretch bending, Journal of Materials Processing Technology 128 (2002) 48-66.

[6] S. Chatti, U. Dirksen, M. Kleiner, Optimization of the design and manufacturing process of bent profiles, Journal of the Mechanical Behaviour of Materials 15 (6) (2004) 437-444.

[7] Y. Okude, S. Sakaki, S. Yoshihara, Improving working limit in draw bending process of aluminum square tubes in large bending radius, Proceedings of the 9th International Conference on Technology of Plasticity, Korea, 2008, 564-569.

[8] T. Kuboki, K. Takahashi, K. Ono, K. Yano, A new schedule-free mandrel-less bending method for straight/pre-shaped long tubes, CIRP Annals-Manufacturing Technology 62 (2013) 303-306.

[9] X.Z. Liu, C.G. Liu, Y. Yao, X.G. Zhang, Numerical analysis for multi-point forming of aluminum alloy profile, Advanced Materials Research 1035 (2014) 128-133.

[10] Z. Gu, M. Lv, X. Li, H. Xu, Stretch bending defects control of L-section aluminum components with variable curvatures, The International Journal of Advanced Manufacturing Technology 85 (2016) 1053-1061.

[11] S. Chatti, M. Hermes, M. Kleiner, Three-dimensional bending of profiles by stress superposition, In: D. Banabic (Ed.), Advanced Methods in Material Forming, Springer Verlag, Berlin, 2007, pp. 101-118.

[12] M. Hermes, S. Chatti, A. Weinrich, A.E. Tekkaya, Three-dimensional bending of profiles with stress superposition, International Journal of Material Forming 1 (1) (2008) 133-136.

[13] M. Hermes, M. Kleiner, Method and device for profile bending, in: European Patent EP2144720B1, 2008.

[14] S. Chatti, M. Hermes, A.E. Tekkaya, M. Kleiner, The new TSS bending process: 3D bending of profiles with arbitrary cross-sections, CIRP Annals-Manufacturing Technology 59 (1) (2010) 315-318.

[15] M. Hermes, D. Staupendahl, M. Kleiner, Torque superposed spatial bending, In: A.E. Tekkaya, W. Homberg, A. Brosius (Eds.), 60 Excellent Inventions in Metal Forming, Springer Verlag, Berlin, 2015, pp. 381-385.

[16] M. Kleiner, D. Arendes, The manufacture of non-linear aluminium sections applying a combination of extrusion and curving, Processings of the 5th International Conference on Technology of Plasticity 2, 1996, pp. 971-974.

[17] A. Selvaggio, D. Becker, A. Klaus, D. Arendes, M. Kleiner, Curved Profile Extrusion, In: A.E. Tekkaya, W. Homberg, A. Brosius (Eds.), 60 Excellent Inventions in Metal Forming, Springer Verlag, Berlin, 2015, pp. 287-292.

[18] K.B. Müller, Bending of extruded profiles during extrusion process, Materials Forum 28 (2004) 264-269.

[19] K.B. Müller, Bending of extruded profiles during extrusion process, International Journal of Machine Tools and Manufacture 46 (11) (2006) 1238-1242.

[20] M. Shiraishi, M. Nikawa, Y. Goto, An Investigation of the Curvature of Bars and Tubes Extruded through Inclined Dies, International Journal of Machine Tools & Manufacture 43 (2003) 1571-1578.

[21] M. Nikawa, M. Shiraishi, Y. Miyajima, H. Horibe, Y. Goto, Production of shaped tubes with various curvatures using extrusion process through inclined die aperture, Journal of the Japan Society for Technology of Plasticity 43 (498) (2002) 654-656.

[22] Y. Takahashi, S. Kihara, K. Yamaji, M. Shiraishi, Effects of die dimensions for curvature extrusion of curved rectangular bars, Materials Transactions 56 (2015) 844-849.

[23] L.D.I. Dajda, Z.D.I. Hranos, Z.D.I. Petrzela, Extrusion of pipe bends and elbow-by means of die with eccentric hole and eccentrically mounted mandrel, in: Deutschen Patent DE2855449A1, 1978.

[24] F.K. Chen, W.C. Chuang, S. Torng, Finite element analysis of multi-hole extrusion of aluminum-alloy tubes, Journal of Materials Processing Technology 201(1) (2008) 150-155.

[25] R. Geiger, W. Schätzle, Grundlagen und Anwendung des QuerflieBpressens [Principles and applications of transverse extrusion], Proceedings of the International Conference on Fundamentals of Metal Forming Technique-State and Trends, Stuttgart, October 1983, pp. 139-160 (in German).

[26] K. Lange, Handbook of metal forming, McGraw-Hill, New York, 1985.

[27] M. Merklein, Cold Forging, In: L. Laperrière, G. Reinhart (Eds.), CIRP Encyclopedia of Production Engineering, Springer Verlag, Berlin, 2014, pp. 226-231.

[28] S. Rudolf, Hollow lateral extrusion of tubular billets-a newly developed cold forging process, In: 43rd plenary meeting of the International Cold Forging Group (ICFG), Darmstadt, Germany, 2010.

[29] J. Wälder, M. Liewald, Hollow lateral extrusion of tubular billets-Further development of the cold forging process, Applied Mechanics and Materials 794 (2015), pp. 160-165.

[30] J.C. Henry, An investigation of the injection upsetting of six steels, NEL Report 494, UK: National Engineering Laboratory, 1971.

[31] R. Balendra, Process mechanics of injection upsetting, International Journal of Machine Tools and Manufacture 25 (1) (1985) 63-73.

[32] R. Geiger, From near-net-shape to net-shape cold forging-state of the art, Processings of the 9th Cold Forging Congress, UK, May 1995, pp. 59-75.

[33] R. Balendra, Y. Qin, Identification and classification of flow-dependent defects in the injection forging of solid billets, Journal of Materials Processing Technology 106 (1-3) (2000) 199-203.

[34] Y. Qin, R. Balendra, Computer-aided design of nett-forming by injection forging of engineering components, Journal of Materials Processing Technology 76 (1-3) (1998) 62-68.

[35] L.M. Alves, P.A.F Martins, Injection forging of solid asymmetric branched components, Proceedings of the Institution of Mechanical Engineers, Part B: Journal of Engineering Manufacture 227 (6) (2013) 898-907.

[36] T. Nakano, Modern applications of complex forging and multiaction forming in cold forging, Journal of Materials Processing Technology 46 (1-2) (1994) 201-226.

[37] W. Johnson, R. Sowerby and R. D. Venter, Plane-Strain Slip-Line Fields for Metal-Deformation Processes, Pergamon Press, UK, 1982, pp. 110.

[38] N. Bay, T. Wanheim, M. Arentoft, C.B. Andersen, B. Bennani, An appraisal of numerical and physical modelling for prediction of metal forming processes, Processings of the 4th International Conference on Computational Plasticity-Fundamentals and Applications, Barcelona, Spain, 1995, pp. 1343-1354.

[39] V. Vazquez, K. Sweeney, D. Wallace, C. Wolff, M. Ober, T. Altan, Tooling and process design to cold forge a cross groove inner race for a constant velocity joint-physical modeling and FEM process simulation, Journal of Materials Processing Technology 59 (1996) 144-157.

[40] H. Sofuoglu, Physical modeling and finite element analysis of friction encountered in large deformation processes, Ph.D. Thesis, Texas Tech University, USA, 1993.

[41] A. Assempour, A. Hassannejadasl, Minimization of the exit profile curvature in non-symmetric T-shaped sections, Materials and Design 30 (2009) 1350-1355.

[42] S.Z. Zhang, Extrusion process and die design, Chemical Industry Press, China, 2009, pp.103.

[43] T. Altan, S.-I. Oh, H.L. Gegel, Metal Forming: Fundamentals and Applications, ASM, Metal Parks, OH 1983.

[44] O. Pawelski, Ways and limits of the theory of similarity in application to problems of physics and metal forming, Journal of Materials Processing Technology 34 (1992) 19-30.

[45] X.J. Duan, T. Sheppard, The influence of the constitutive equation on the simulation of a hot rolling process, Journal of Materials Processing Technology 150 (2004) 100-106.

[46] T. Altan, F. W. Boulger, Flow stress of metals and its application in metal forming analyses, ASME Journal of Engineering for Industry 95 (1973) 1009-1019.

[47] M. El Mehtedi, S. Spigarelli, F. Gabrielli, L. Donati, Comparison study of constitutive models in predicting the hot deformation behavior of AA6060 and AA6063 Aluminium alloys, Materials Today: Proceedings 2 (2015) 4732-4739.

[48] Z.Y. Jiang, X.L. Liu, X.H. Liu, G.D. Wang, Analysis of ribbed-strip rolling by rigid-viscoplastic FEM, International Journal of Mechanical Sciences 42 (2000) 693-703.

[49] S.W. Xiang, G.D. Wang, Q. Zhang, A new model for deformation resistance, Journal of Iron and Steel 28(5) (1993) 21-26.

[50] T. Sheppard, A. Jackson, Constitutive equations for use in prediction of flow stress during extrusion of aluminium alloys, Materials Science and Technology 13 (3) (1997) 203-209.

[51] G. Liu, J. Zhou, J. Duszczyk, Finite element simulation of magnesium extrusion to manufacture a cross-shaped profile, ASME Journal of Manufacturing Science and Engineering 129 (2007) 607-614.

[52] E.A. El-Danaf, Mechanical properties and microstructure evolution of 1050 aluminum severely deformed by ECAP to 16 passes, Materials Science and Engineering A 487 (2008) 189-200.

[53] Y. Iwahashi, Z. Horita, M. Nemoto, T.G. Langdon, An investigation of microstructural evolution during equal-channel angular pressing, Acta Materialia 45 (1997) 4733-4741.

[54] D. N. Lee, An Upper-Bound Solution of Channel Angular Deformation, Scripta Materialia 43 (2000) 115-118.

Figures and Tables

Table 1 Dimensions of the DVSE tooling, specific extrusion process parameters

	D_2 (mm)	D_3 (mm)	t (mm)	λ
Round bar	20	-	-	1.61
	15	-	-	2.87
Round Tube	15	7	4	3.67
	15	9	3	4.48
	15	11	2	6.20
	20	11	4.5	2.31
	20	13	3.5	2.79
	20	15	2.5	3.69

(D_2: diameter of the die exit orifice; D_3: diameter of the mandrel; t: extrudate thickness; λ: extrusion ratio)

Table 2 Norton-Hoff coefficients for the flow stress of plasticine.

K (10^8 N/mm^2)	β	n	m
1.8	0.07	0.15	0.14

Table 3 Thermal properties of the billet and extrusion tooling.

Property	AA6082	H13 tool steel
Heat capacity(N/(mm^2·^{o}C))	2.43328	2.8 at 93 ^{o}C 3.2 at 315 ^{o}C 4.5 at 538 ^{o}C
Thermal conductivity (N/(s·^{o}C))	180.195	24
Heat transfer coefficient between tooling and billet (N/(mm·s·^{o}C))	11	11
Heat transfer coefficient between tooling/billet and air (N/(mm·s·^{o}C))	0.02	0.02
Emissivity	0.7	0.7

Table 4 Material constants for AA6082.

$1/\alpha$ (N/mm^2)	Q (10^5 J/mol)	R (J/(K·mol)	A (10^8/s)	n
22.2	1.53	8.314	2.39	2.976

(a) Curved profile extrusion (CPE) [17]

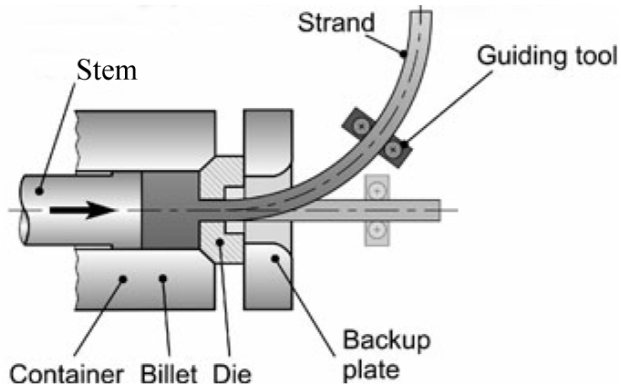

(b) Curved profile extrusion (CPE) [19]

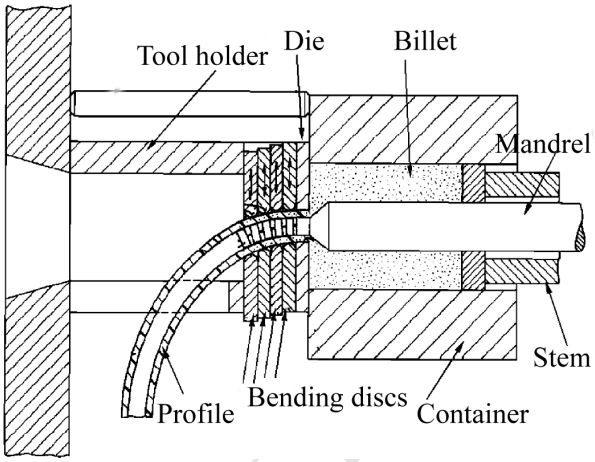

(c) Inclined die orifice extrusion [20]

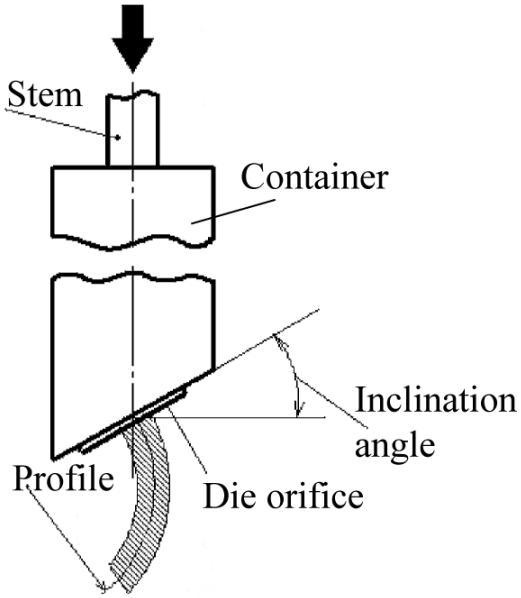

(d) Multi-hole extrusion [24]

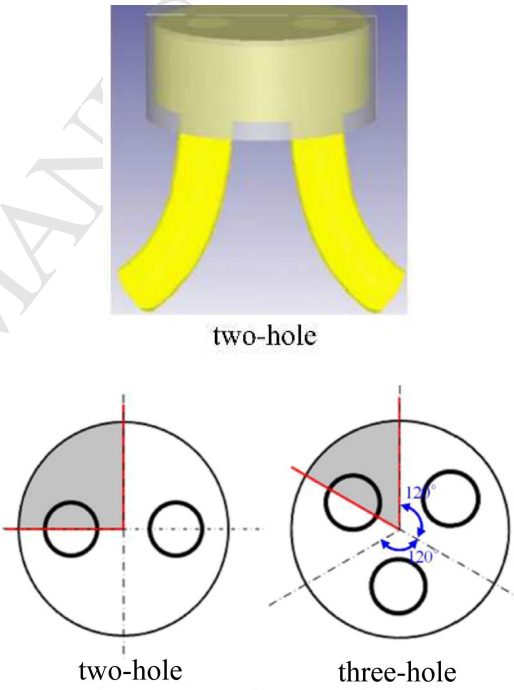

Fig. 1. Illustration of process principles of extrusion-bending integrated methods which are based on external bending apparatus [17,19] and extrusion tooling designs [20,24] to influence material flow**.**

(a) Radial extrusion [27]

(b) Radial extrusion [28,29]

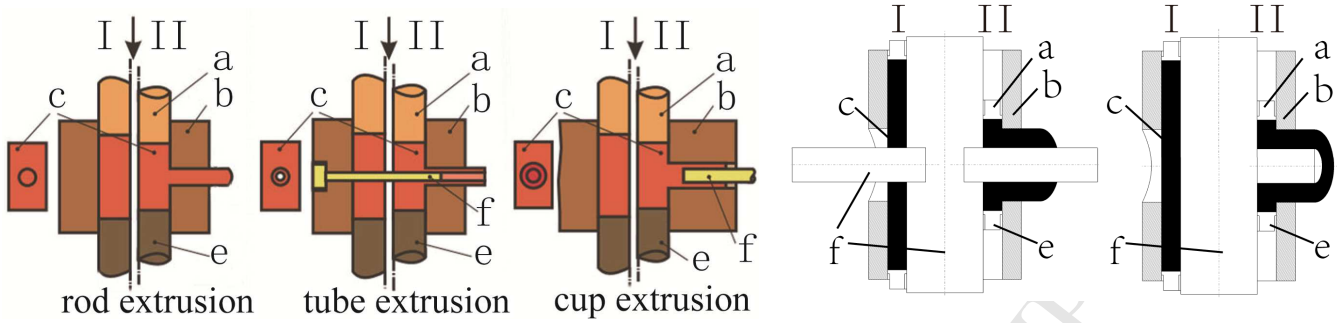

(c) Radial forging [34]

(d) Radial forging [35]

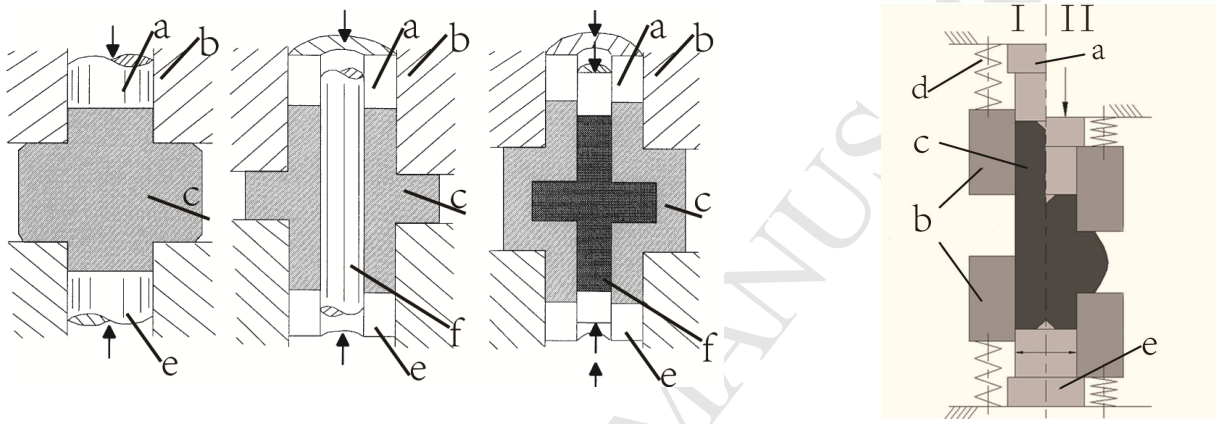

Fig. 2. Illustrations of the radial extrusion [27-29] and radial forging [34,35] processes: I-prior to extrusion/forging; II-after extrusion/forging; a-punch; b-container; c-workpiece; d-spring; e-counterpunch; f-mandrel.

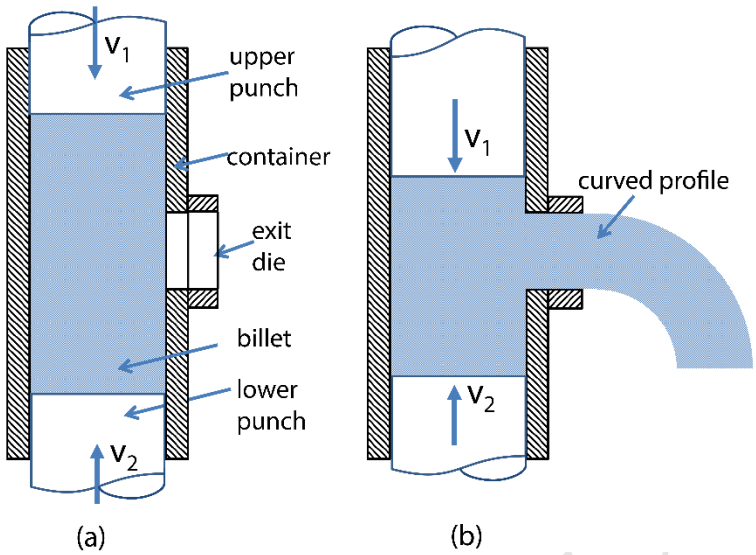

Fig. 3. Schematic illustration of differential velocity sideways extrusion (DVSE): (a) initial stage, (b) intermediate stage.

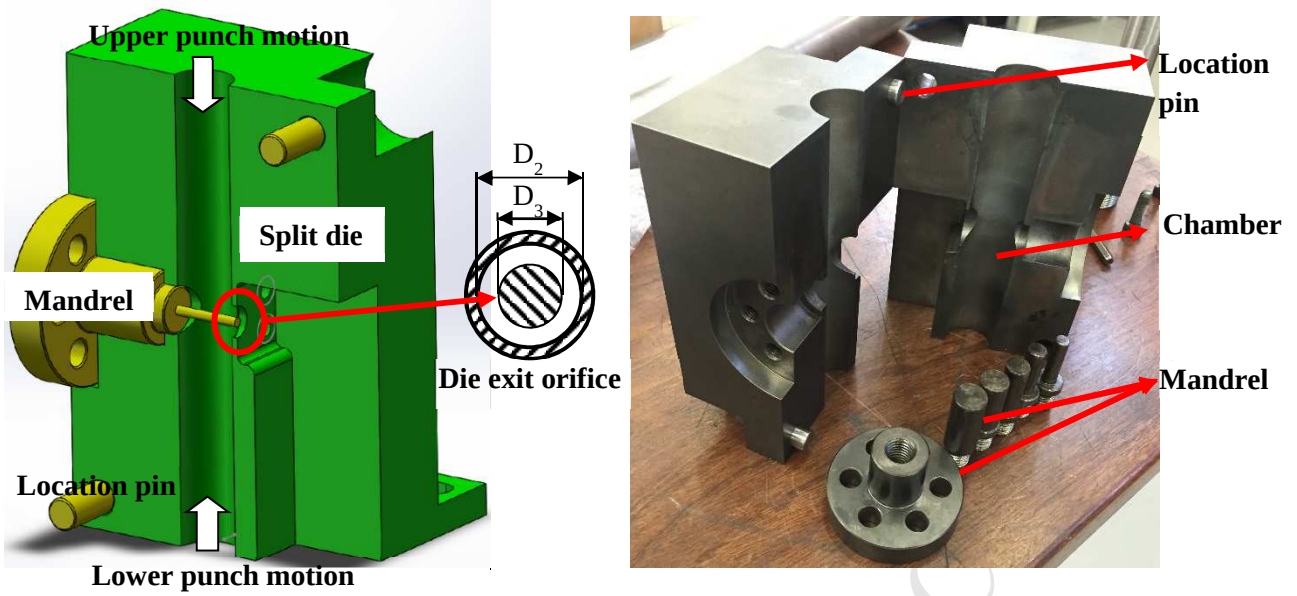

(a)

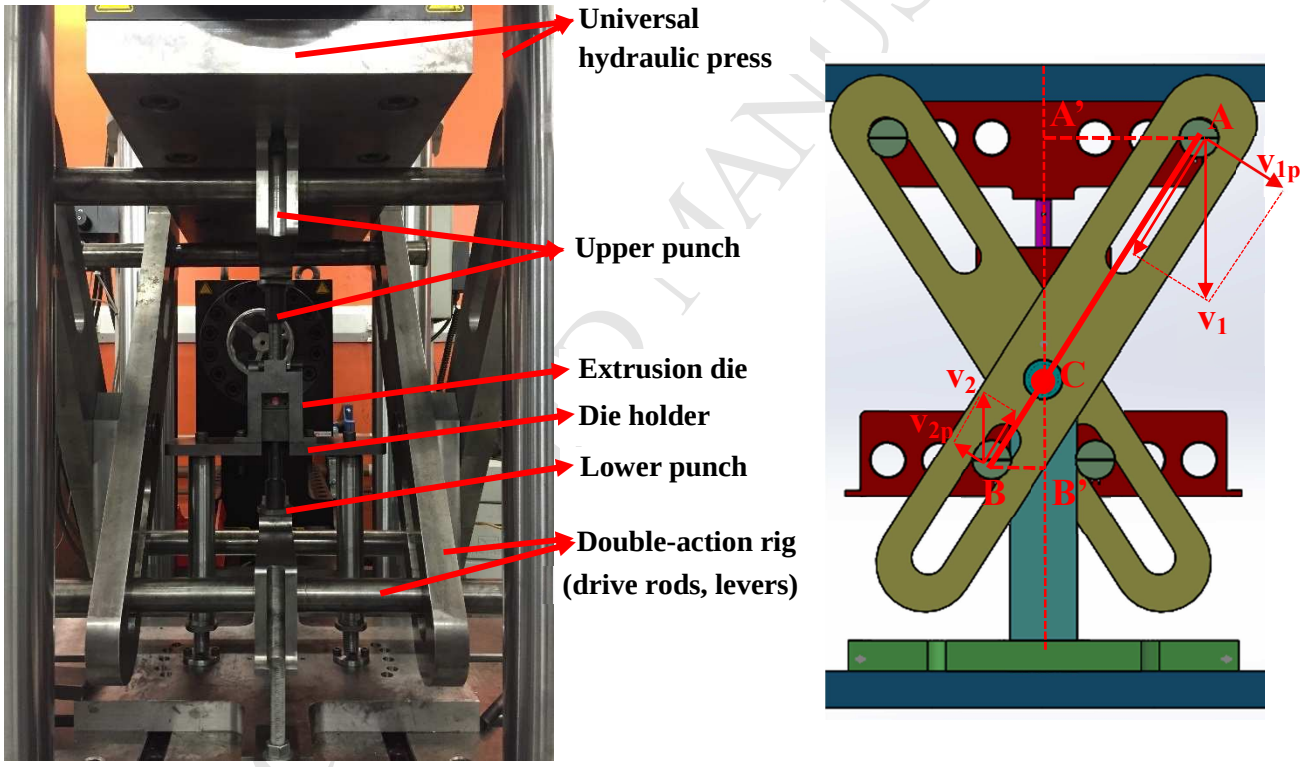

(b) (c)

Fig. 4. (a) Designed and manufactured split extrusion die, (b) extrusion die and double-action loading rig assembled and centralized on the 2500kN Instron universal hydraulic press, (c) illustration of the kinematics of the double-action loading rig.

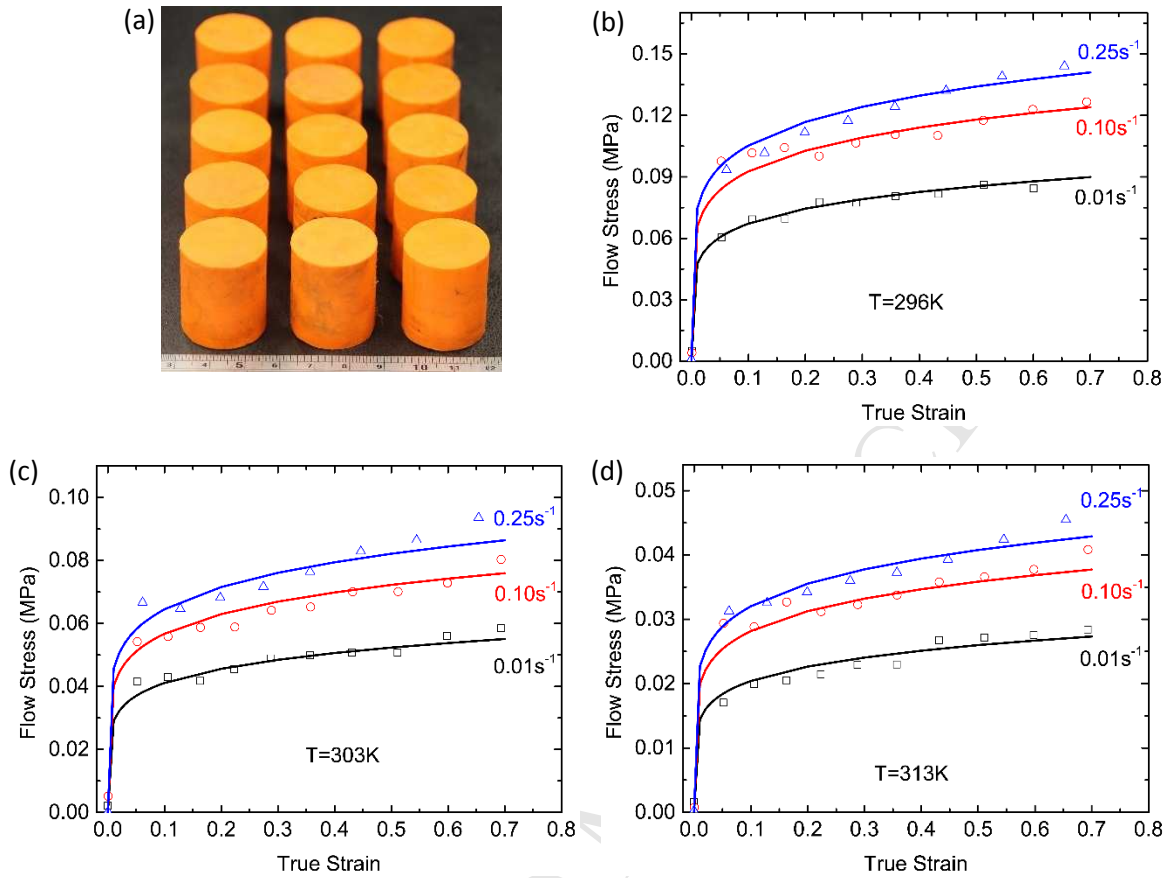

Fig. 5. (a) Plasticine samples; Comparison of experimental (hollow symbols) and Norton–Hoff fitted (solid curves) true stress-strain curves of plasticine at strain rates of 0.01-0.25s^{-1} and temperatures of (b) 296 K, (c) 303 K, and (d) 313 K.

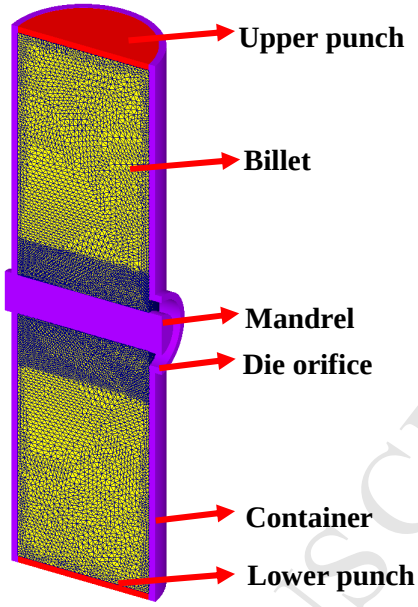

Fig. 6. FE model of DVSE fabricating curved round tubes.

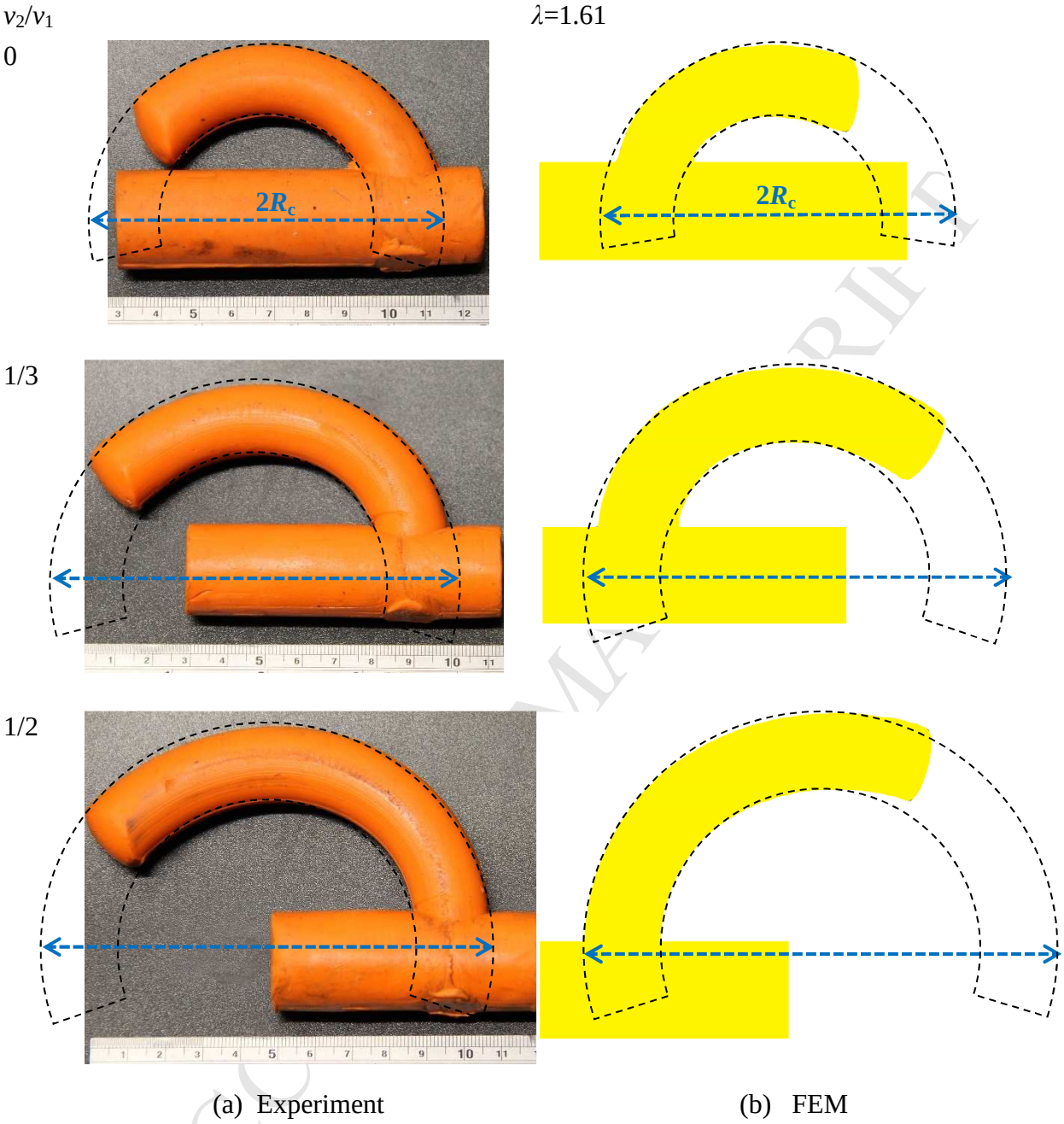

Fig. 7. Comparison between (a) experimental and (b) FEM results for bars extruded at extrusion ratio λ=1.61 and extrusion velocity ratios v_2/v_1=0, 1/3, 1/2.

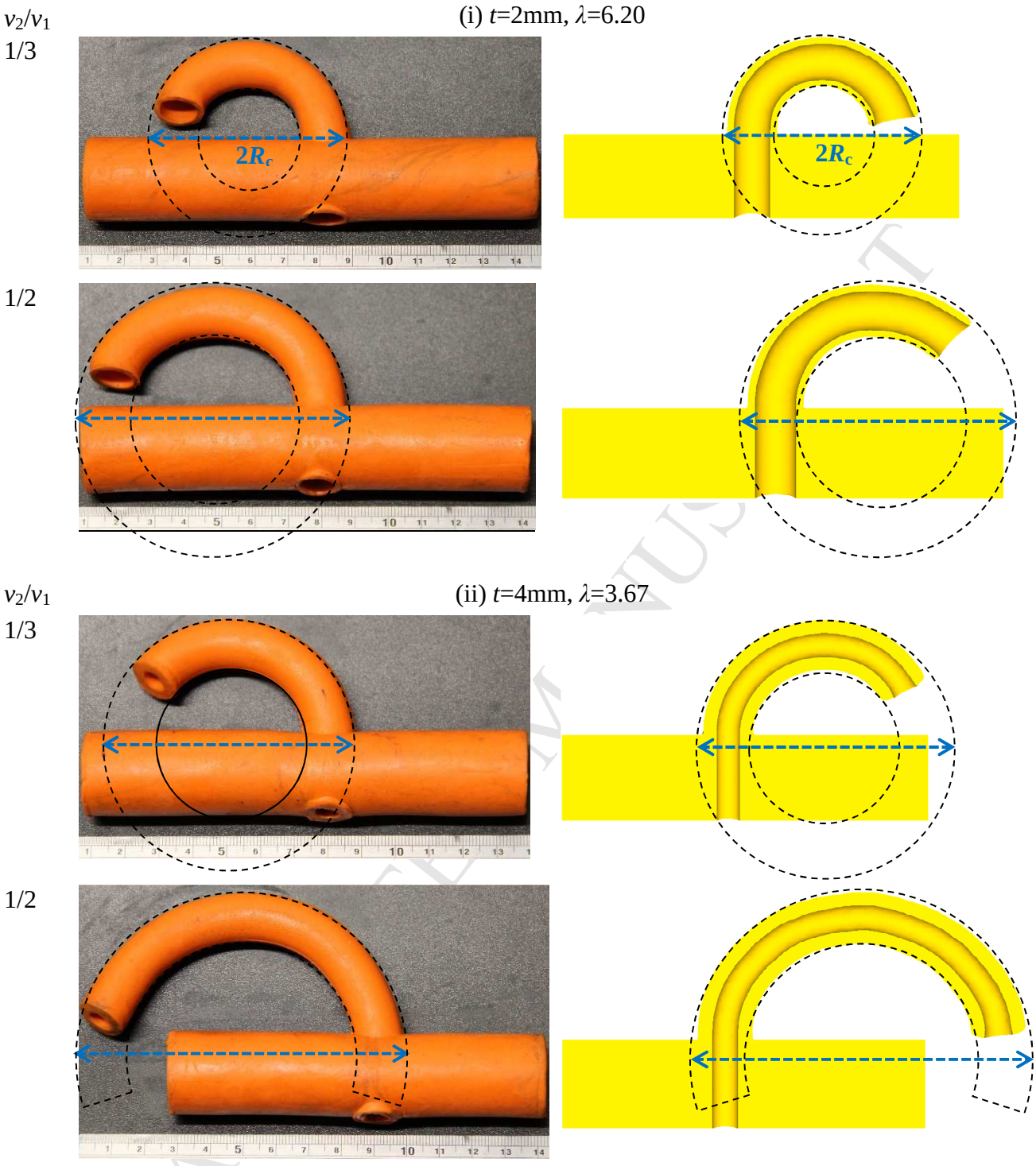

Fig. 8. Comparison between (a) experimental and (b) FEM results for tubes extruded at extrusion velocity ratios v_2/v_1=1/3, 1/2, extrusion ratios λ=6.20 (thickness 2mm) and λ=3.67 (thickness 4mm).

Fig. 9. Trial tests using commercial pure aluminium AA1050

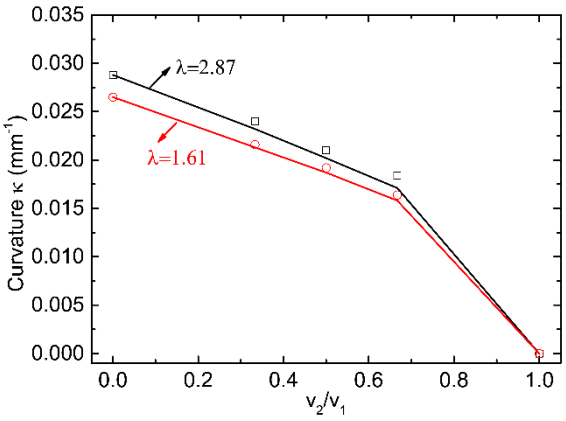

(a) Solid bars

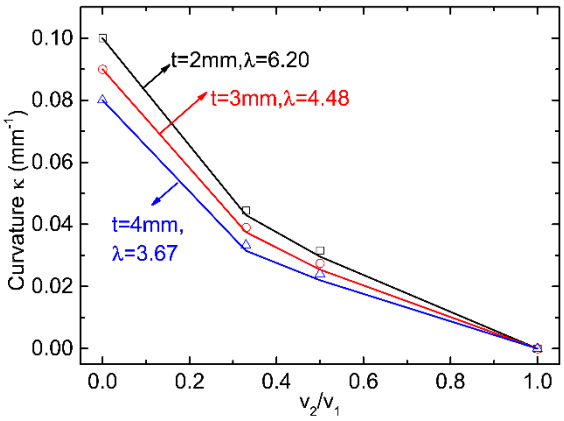

(b) Tubes with outside diameter D_2=15mm

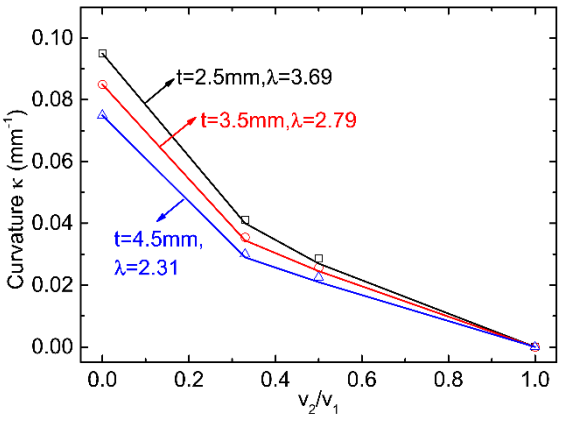

(c) Tubes with outside diameter D_2=20mm

Fig. 10. Comparison of curvature variations for the results obtained from experiment (hollow symbols) and FEM (solid curves).

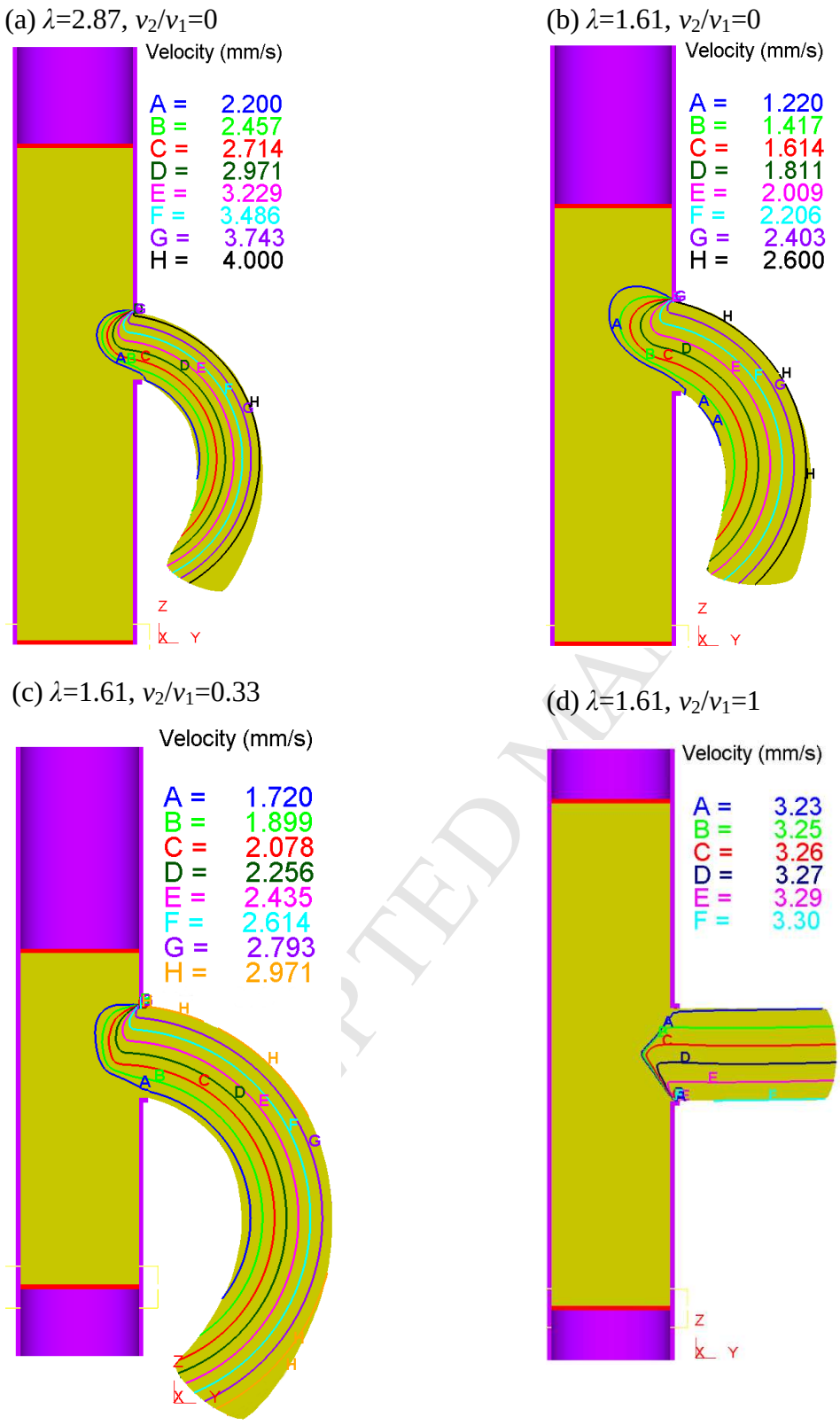

Fig. 11. Material flow velocity distribution of extruded bars at the die exit orifice.

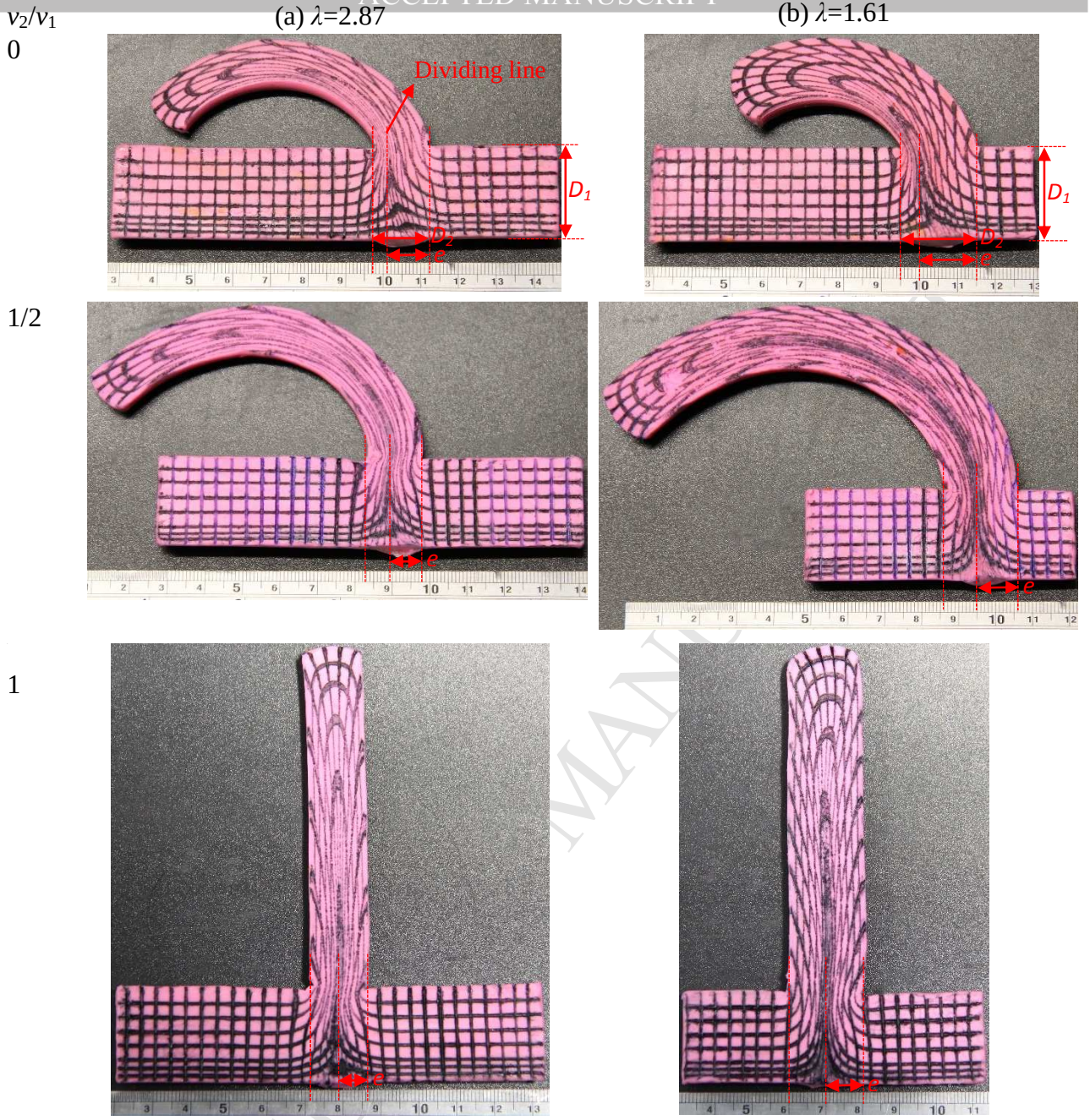

Fig. 12. Distorted grids on extruded bars.

(a) λ=2.87, v_2/v_1=0

(b) λ=1.61, v_2/v_1=0

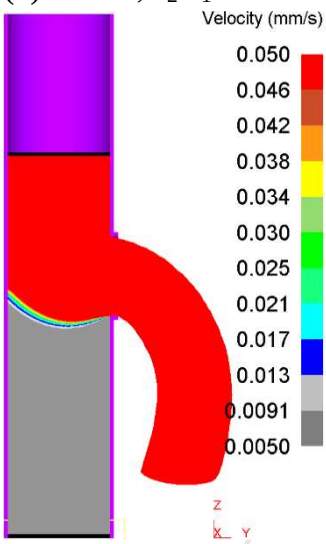

(c) λ=1.61, v_2/v_1=0.33

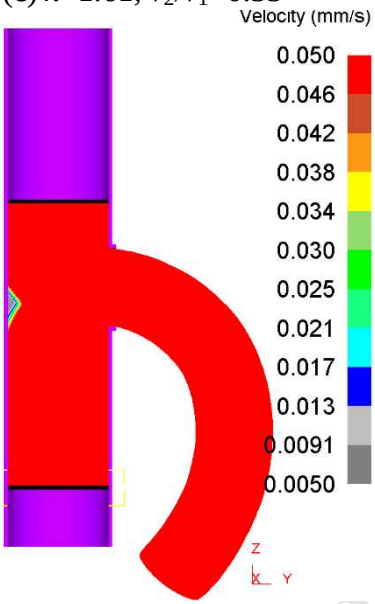

(d) λ=1.61, v_2/v_1=1

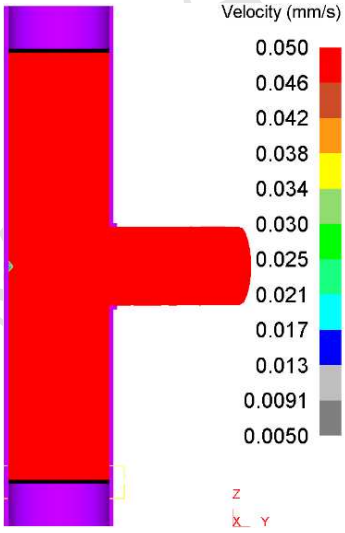

Fig. 13. Simulations showing dead zones in extruded bars.

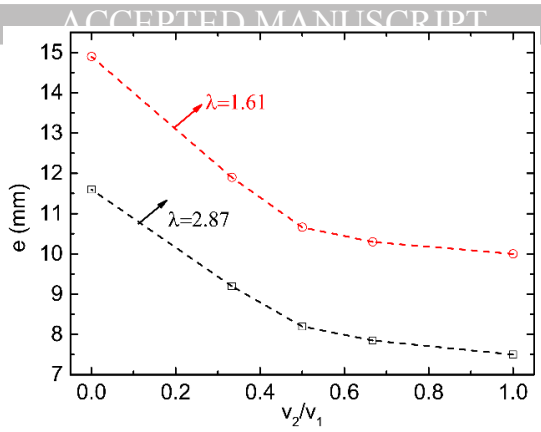

(a) e

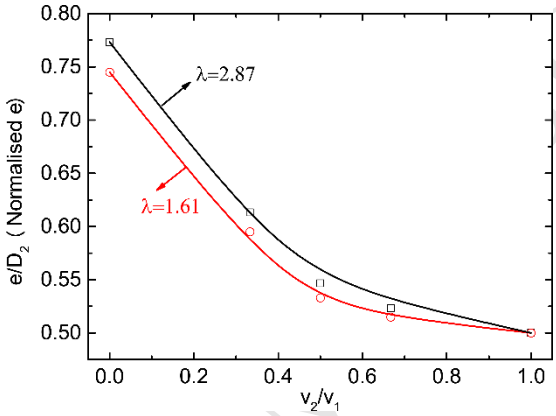

(b) Eccentricity ratio $\hat{e} = e/D_2$

Fig. 14. Variations of (a) e and (b) eccentricity ratio $\hat{e} = e/D_2$ (experiment-hollow symbols, FEM-solid curves) with different extrusion velocity ratios and extrusion ratios.

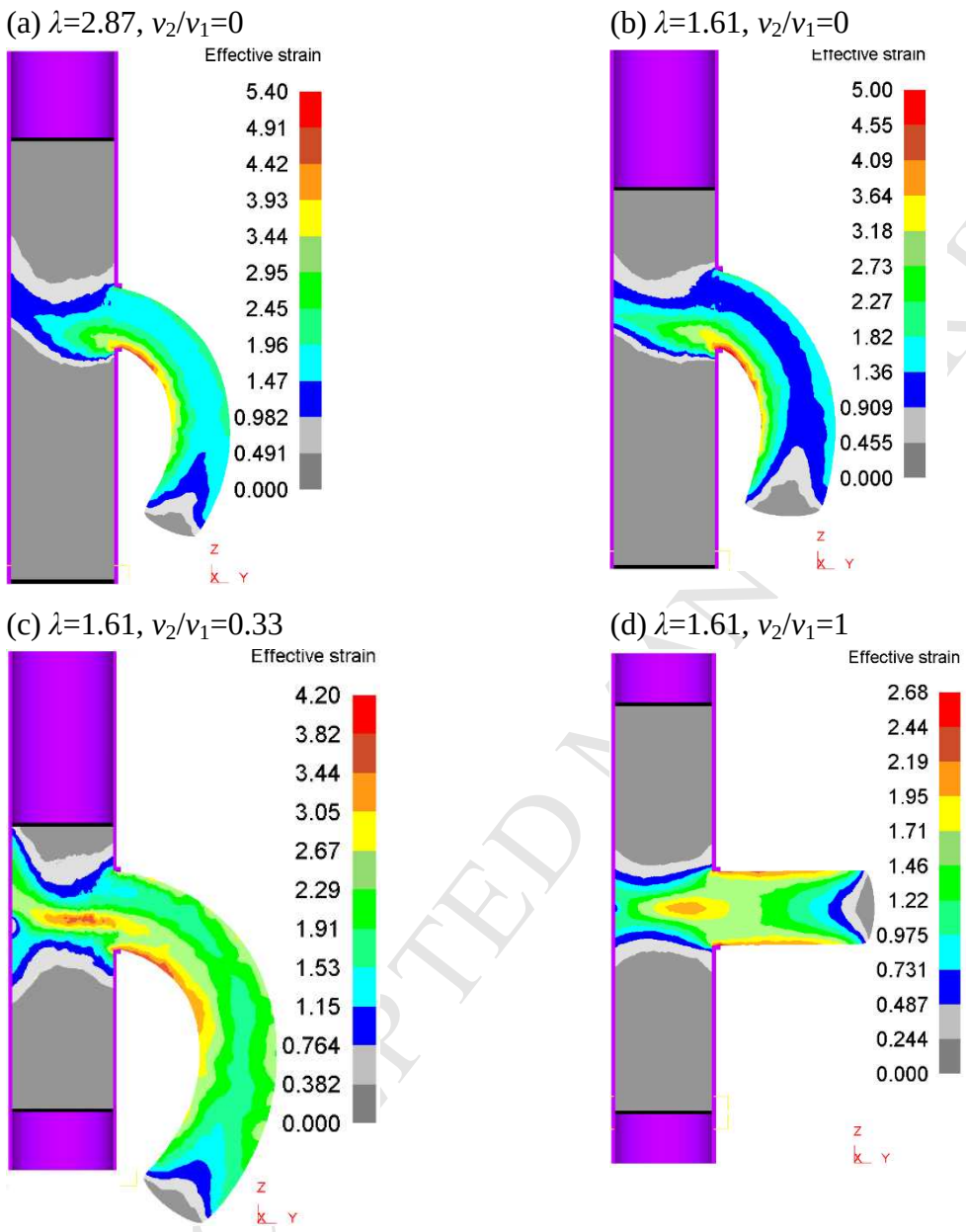

Fig. 15. Effective strain contours of extruded bars with different extrusion velocity ratios and extrusion ratios.

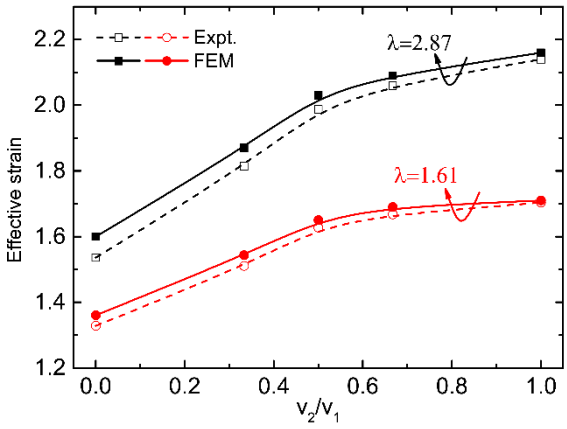

Fig. 16. Comparison of effective strain of the outside bending region of the profile obtained from experiment (hollow symbols and dash curves) and FEM (solid symbols and solid curves).

Highlights

•A novel process, differential velocity sideways extrusion (DVSE), for manufacturing curved profiles was studied by a designed tool set.

•DVSE can efficiently form billets into curved profiles without defects in one procedure.

•Curvatures can be actively controlled by the velocity ratio of extrusion punches and the extrusion ratio.

•Severe plastic deformation occurs in DVSE and profiles have greatly promoted effective strain levels.